

# Fullerene C<sub>60</sub> Formation in Partially Ionized Carbon Vapor

G. N. Churilov, A. S. Fedorov, and P. V. Novikov

Kirenskii Institute of Physics, Siberian Division, Russian Academy of Sciences,  
Akademgorodok, Krasnoyarsk, 660036 Russia

e-mail: churilov@iph.krasn.ru

Received July 24, 2002; in final form, September 23, 2002

The assembling rate of a fullerene C<sub>60</sub> molecule has been theoretically studied as a function of electron concentration and temperature in partially ionized carbon vapor. For C<sub>60</sub> formation via one or two intermediate stages of cluster collisions, it has been shown that there is a region of plasma parameters (the temperature and electron concentration) in which fullerene C<sub>60</sub> is formed more efficiently. The C<sub>60</sub> formation rate versus temperature and electron concentration relationships have been found to correlate with the trends in the collision cross-section of carbon clusters as functions of these parameters. © 2002 MAIK “Nauka/Interperiodica”.

PACS numbers: 52.27.Lw; 52.20.Hv; 36.40.Gk

Numerous studies are known to concern fullerene formation upon condensation of carbon vapor, but the mechanism of formation is not fully clear [1]. Fullerene formation is, as a rule, considered in electroneutral carbon vapor and not in carbon-containing plasma. Therefore, the role of the carbon-cluster charge in cluster joining was ignored, although it is known from experiments that charged particles affect fullerene formation [2]. Alekseev and Dyuzhev [3] considered the effect of carbon-cluster charge on carbon-structure formation. They inferred that plasma parameters affect the spatial cluster-charge distribution in the plasma jet and the conditions for plasma discharge. However, the effect of the cluster charge on the fullerene formation rate has not been touched in that study.

Our purpose in this work was to quantify the effect of the carbon-cluster charge on the formation rate of fullerene C<sub>60</sub> as a function of the electron concentration and temperature of carbon–helium plasma. We have shown that the charge on carbon clusters (which substantially changes the collision cross-section of clusters and, in association, the fullerene formation rate) should be included into the consideration of fullerene formation. The cluster charge is a function of electron concentration  $n_e$  and temperature  $T$  in plasma. The  $n_e$  and  $T$  parameters were believed to be independent of each other in the calculations of the carbon subsystem. Although the plasma parameters should be calculated self-consistently, doping the plasma with small amounts of electron donors (acceptors) is an efficient means for changing the electron concentration at a given temperature; thus these parameters become in fact independent of each other. Particular routes of C<sub>60</sub> assembling and C<sub>60</sub> isomerization to yield fullerene were beyond the scope of this study; these points have been considered elsewhere.

One of the basic postulates that are employed in most studies dealing with fullerene formation in plasma arc is that the plasma is considered as occurring in the state of local thermodynamic equilibrium. If this is the case, Saha's equations are applicable to determine cluster-charge distribution in partially ionized carbon vapor for different values of electron concentration  $n_e$  and temperature  $T$ . The calculations were applied to the carbon–helium plasma under atmospheric pressure (with 10<sup>2</sup> Pa partial carbon pressure) for the temperature range 1500–5000 K; the range of fullerene formation temperatures falls within this range [4]. We ignored a reduction in the fullerene formation rate at lower temperatures caused by decreases in the carbon evaporation rate and the cluster-isomerization rate. Taking this factor into account would have reduced the relationship for the fullerene appearance rate at lower temperatures of  $T < 2000$  K (Figs. 2, 3).

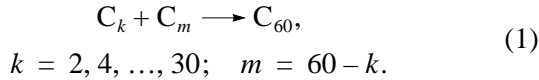
We assumed that the fullerene C<sub>60</sub> yield is proportional to the formation rate of fullerene molecules. This assumption might be proven by the fact that fullerene molecules are stable and have high bond energies, and their transformation to other clusters (having another mass) is inessential compared to their formation. To find the cluster-collision frequency, the scattering cross-sections derived from classical collision theory were used. Classical theory is useful for finding the scattering cross-sections due to the fact that carbon clusters have large masses compared to the electron mass. The ionization potentials and electron affinities of carbon clusters were found from *ab initio* quantum-chemical calculations.

A null activation barrier to the joining reaction of any clusters was assumed in the calculations; that is, the collision of any two clusters C<sub>*k*</sub> and C<sub>*m*</sub> resulted in the appearance of cluster C<sub>*k+m*</sub>. This assumption is based

on the common chemical character of colliding clusters, which leads to small variations in the activation barrier. Another base is the fact that, upon averaging the colliding clusters with respect to their shape and mutual position, the barriers of joining reactions should tend to a constant value. Any fixed barrier to joining for all clusters cannot change the results of the calculation apart from introducing a common normalizing factor. For simplicity, this factor was ignored.

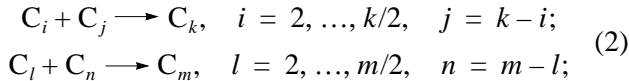
Only reactions between clusters containing an even number of atoms were included into the calculations; in experiments [5], the mass-spectrometric analysis of carbon clusters during fullerene formation showed that even-atom clusters in plasma are several orders of magnitude more abundant than odd-atom clusters.

We considered the final process of C<sub>60</sub> assembling in one and two reaction stages. In the one-stage process, reactions between all possible pairs of carbon clusters that result in molecule C<sub>60</sub> were considered. Clearly, the sum of the masses of colliding clusters is equal to the mass of molecule C<sub>60</sub>:

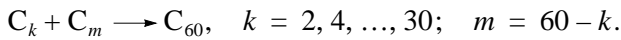


In the two-stage process, in addition to all reactions of C<sub>60</sub> formation from clusters C<sub>k</sub> and C<sub>m</sub>, all reactions that yield these clusters C<sub>k</sub> and C<sub>m</sub> were considered.

For stage 1:



For stage 2:



Introduction of the cluster-size distribution function was an important point of the calculations. Several distribution functions were used. The basic distribution used corresponded to the cluster-mass distribution from [6]. The other two distributions were chosen from [7]. For all of the distributions used, the C<sub>60</sub> formation rate versus electron concentration and versus temperature relationships were the same. Therefore, the data derived are applicable to an experiment in which the cluster distribution function is not steady-state.

The focus of our approach is the calculation, from gas theory [9], of the rate  $R_{km}(q_k, q_m)$  of the collision (that results in joining) of two clusters C<sub>k</sub> and C<sub>m</sub> bearing charges  $q_k$  and  $q_m$ , respectively:

$$R_{km}(q_k, q_m) = n_m(q_m)n_k(q_k)v_{km}\sigma_{km}(q_k, q_m). \quad (3)$$

Here,  $n_m(q_m)$  and  $n_k(q_k)$  are the concentrations of clusters C<sub>k</sub> and C<sub>m</sub> that bear charges  $q_k$  and  $q_m$ ,  $v_{km} = \sqrt{8k_B T / \pi m_{km}}$  is the mean rate of the relative movement of these clusters,  $m_{km} = m_k m_m / (m_k + m_m)$  is the normal-

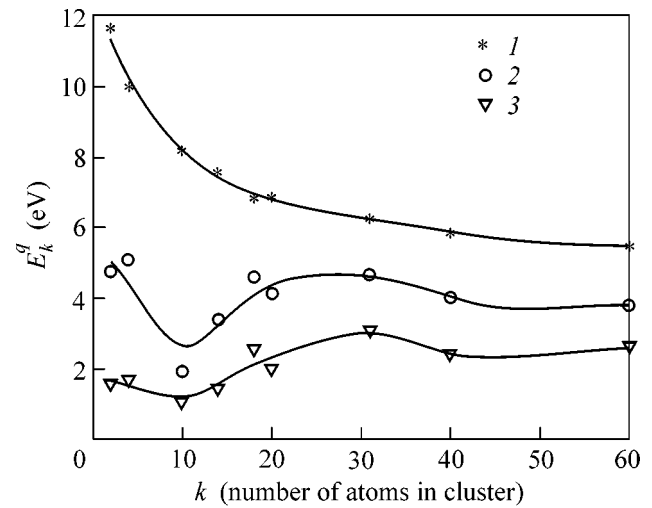


**Fig. 1.** Plots of (1) the ionization potential  $E_k^0$ , (2) electron affinity  $-E_k^{-1}$ , and (3) electron affinity of the anion  $-E_k^{-2}$  for the carbon clusters used in the calculations.

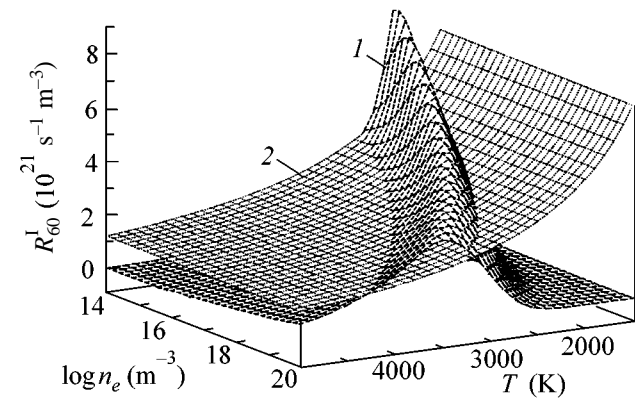


**Fig. 2.** Plots of (1) the fullerene C<sub>60</sub> formation rate in one stage and (2) C<sub>60</sub> formation rate in one stage from neutral clusters.

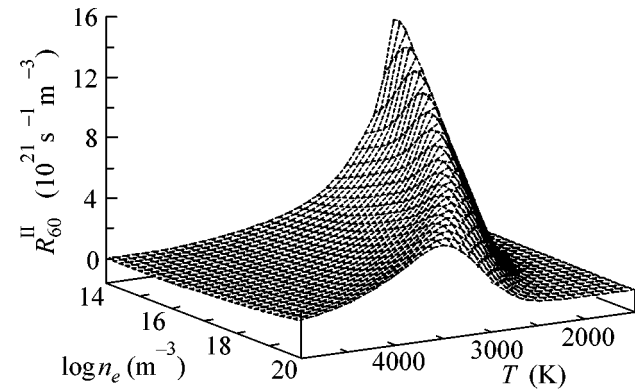


**Fig. 3.** Fullerene C<sub>60</sub> formation rate in the two-stage process.

ized mass of the clusters, and  $\sigma_{km}(q_k, q_m)$  is the collision cross-section of these particles.

From classical collision theory, the effective collision cross-section of charged particles [10] is defined as

$$\sigma_{km}(q_k, q_m) = \sigma_{km}^0 \left( 1 - \frac{q_k q_m e^2}{r_{km} \epsilon_{kin}} \right). \quad (4)$$

Here,  $\sigma_{km}^0 = \pi r_{km}^2$  is the collision cross-section of neutral clusters  $C_k$  and  $C_m$ ,  $r_{km} = r_k + r_m$  is the impact distance between two clusters, and  $q_k q_m e^2 / r_{km} \epsilon_{kin}$  is the ratio of the electrostatic and mean kinetic energies  $\epsilon_{kin} = 3/2 k_B T$  of the relative cluster movement.

The effective radius  $r_k$  of cluster  $C_k$  was always set equal to  $r_k = 1/2(d_x d_y d_z)^{1/3}$ , a value equal to one-half cube root of the product of the three maximal dimensions  $d_x$ ,  $d_y$ , and  $d_z$  of the cluster. This distance was calculated for the basis set of clusters of different sizes and shapes:  $C_2$  and  $C_4$  are chains,  $C_{10}$  is a ring,  $C_{14}$  and  $C_{18}$  are planar clusters composed of hexagons,  $C_{20}$  is a cup shaped as a coranulene molecule,  $C_{32}$  is a cup composed of pentagons and hexagons,  $C_{40}$  is a cup, fullerene, and fullerene with a heptagon, and  $C_{60}$  is a fullerene and a fullerene with a heptagon [7, 11]. The clusters containing heptagons were included into the calculation because of the important role they play in fullerene formation [8]. For the other clusters  $C_k$  with  $k = 2, \dots, 60$ , radius  $r_k$  was calculated using interpolation of the  $r_k$  of the basis set.

From the relationship above, it is clear that for charges of opposite signs ( $q_1 q_2 < 0$ ), there exists additional attraction between clusters:  $\sigma_{12} > \sigma_0$ , but for similar charges ( $q_1 q_2 > 0$ ) the collision cross-section is smaller:  $\sigma_{12} < \sigma_0$ . When the Coulombic repulsion of two clusters surpasses the kinetic energy of both clusters ( $q_k q_m e^2 / r_{km} \epsilon_{kin} > 1$ ), no collision occurs; in this case,  $\sigma_{12} = 0$ .

It is worth noting that, in view of the high C–C bond energy ( $E_{C-C} = 6.24$  eV), the cluster-dissociation frequency  $\nu_{diss}$  is insignificant with respect to the cluster-joining frequency  $\nu_{join}$ . The cluster-joining frequency in our calculations is estimated at  $\nu_{join} = 10^5$  s<sup>-1</sup>. The dissociation frequency can be estimated from  $\nu_{diss} = \nu_{vib} f(T) \exp(-E/k_B T)$  [12], where  $\nu_{vib}$  is the characteristic vibrational frequency of the cluster (equal to  $10^{11}$  to  $10^{12}$  s<sup>-1</sup>),  $E = N E_{C-C}$  is the activation barrier to cluster dissociation ( $N$  is the number of dissociating bonds), and  $f(T)$  for molecules is  $10^2$ – $10^3$ . For example, given two C–C bonds dissociate, the cluster dissociation frequency is  $\nu_{diss} \approx 10^{-2}$  s<sup>-1</sup>. In view of the above data, cluster dissociation was ignored in the calculations.

The full rate of cluster  $C_{k+m}$  formation from clusters  $C_k$  and  $C_m$  was determined as the sum of the reaction

rates between these clusters with all possible charges:

$$R_{km} = \sum_{q_m = -2}^{+1} \sum_{q_k = -2}^{+1} R_{km}(q_m, q_k). \quad (5)$$

Charges of  $q_i = \{-2, -1, 0, 1\}$  were used for all of the clusters considered; the calculations showed that, for all clusters from the basis set, the affinity for the third electron was negative and the second ionization potential was too high. For example, for ring cluster  $C_{10}$ , coranulene-type cluster  $C_{20}$ , and fullerene  $C_{60}$ , the second ionization potential was 19.85, 19.60, and 17.06 eV, respectively. Therefore, the existence probability of clusters with charges higher than +1 or lower than -2 in plasma discharge is negligible.

Charge distributions  $p_k(q)$  for each cluster  $C_k$ , which show the existence probability of cluster  $C_k$  with charge  $q$ , were defined from Saha's equations

$$\frac{p_k(q+1)n_e}{p_k(q)} = 2a(T) \frac{Z_k^{q+1}}{Z_k^q} \exp\left(-\frac{E_k^q}{k_B T}\right), \quad (6)$$

Here  $a(T) = (m_e k T / 2\pi \hbar^2)^{3/2}$ ,  $n_e$  is the plasma electron concentration,  $E_i^q$  is the ionization potential of cluster  $C_{k+m}^q$ ,

$$Z_k^q(T) = \sum_{n=1}^{n_{max}} g_n \exp\{-(\epsilon_n - \epsilon_1)/k_B T\}$$

is the electron partition function for cluster  $C_k$  with charge  $q$  at temperature  $T$ , and  $g_n$  is the degeneration multiplicity of the electron level  $\epsilon_n$  of cluster  $C_k$ .

Imposing the normalization condition  $p_k(-2) + p_k(-1) + p_k(0) + p_k(+1) = 1$ , the equilibrium concentrations of clusters  $C_k$  with different charges are

$$n_k(q) = n_k p_k(q), \quad q = -2, -1, 0, +1. \quad (7)$$

The mean charge on cluster  $C_k$  in the plasma with electron concentration  $n_e$  and temperature  $T$  was defined from

$$\langle q_k \rangle = \frac{1}{n_k} \sum_{q=-2}^{+1} q n_k(q) = \sum_{q=-2}^{+1} q p_k(q). \quad (8)$$

With this, the overall formation rate  $R_{km}$  (5) of cluster  $C_{k+m}$  upon joining of two other clusters  $C_k$  and  $C_m$  can be expressed as the product of two values, one being a function of cluster charges and the other being not:  $R_{km} = R_{km}^0 P_{km}$ , where  $R_{km}^0 = n_m n_k \nu_{km} \sigma_{km}^0$  is the reaction rate in the case where all clusters are electroneutral, and

$$P_{km} = \sum_{q_m = -2}^{+1} \sum_{q_k = -2}^{+1} p_m(q_m) p_k(q_k) \left( 1 - \frac{q_k q_m e^2}{r_{km} \epsilon} \right). \quad (9)$$

The existing unknown values of ionization potentials  $E_k^0$ , electron affinity  $-E_k^{-1}$ , and electron affinity of the anion  $-E_k^{-2}$  for each cluster  $C_k$  from  $C_2$  to  $C_{58}$  were calculated using interpolation of energies  $E_k^q$  for the basis set of clusters (Fig. 1). Energies  $E_k^q$  for clusters  $C_{40}$  and  $C_{60}$  from the basis set were found by averaging over their isomers.

The VASP program package [13, 14] was used to calculate energies  $E_k^q$ . In this *ab initio* package, in terms of density functional theory (DFT), the plane-wave expansion of wavefunctions and Vanderbilt's pseudopotential [15] for each atom are used, which abruptly speeds up the calculation of the full energy of the system.

From the equations above, one can calculate the assembling rate of a fullerene  $C_{60}$  molecule. The rate of the one-stage process (1) of fullerene  $C_{60}$  formation was found by summation of rates (5) over all  $k$  and  $m$ :

$$R_{60}^I = \sum_{k=2}^{30} R_{k,60-k}. \quad (10)$$

The one-stage assembling rate of  $C_{60}$  at different electron densities and temperatures is imaged by surface 1 in Fig. 2. Surface 2 in the same figure refers to a one-stage process with charges ignored. A fundamental difference is seen to exist between the assembling rates from neutral and charged clusters.

The two-stage assembling rate (process (2)) is mapped in Fig. 3. In mapping, additional concentrations of various clusters  $C_k$  accumulated during the period of time  $\tau = 10^{-5}$  s (chosen to be equal to the mean collision time of carbon clusters with one another) were taken into account:

$$\Delta n_k = \sum_{i+j=k} R_{ij}\tau.$$

Then, in the first order of  $\Delta n_m$  and with  $\Delta n_m \Delta n_k$  terms ignored, the overall two-stage  $C_{60}$  assembling rate is calculated as

$$R_{60}^{II} = R_{60}^I + \sum_{m+k=60} (\Delta n_m n_k + n_m \Delta n_k) v_{km} \sigma_{km}^0 P_{km}. \quad (11)$$

From the similarity of relationships for the assembling rates in one stage (Fig. 2, surface 1) and two stages (Fig. 3), we believe that a similar relationship holds for many (more than two) joining stages. Therefore, the general relationship between the  $C_{60}$  assembling rate and the plasma parameters is expected to be similar to Figs. 2 and 3.

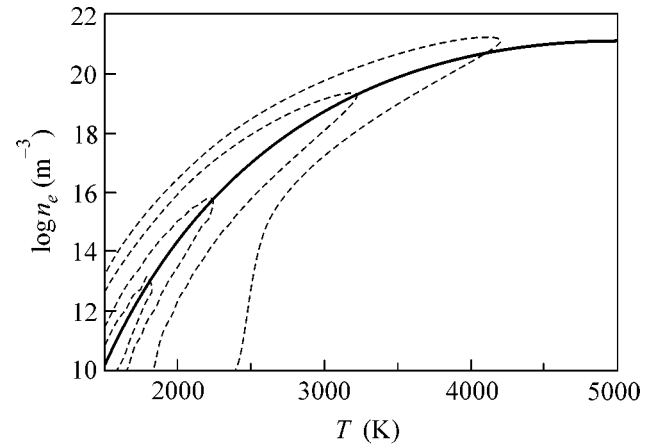


Fig. 4. Plots of the electron concentration vs. temperature for pure carbon-helium plasma  $n_e(T)$  and the envelope plot of the one-stage  $C_{60}$  formation rate.

Figures 2 and 3 make it clear that, for different temperatures, a peak in the  $C_{60}$  formation rate is observed at different electron concentrations. For example, at  $T \sim 2000$  K the peak is observed at  $n_e \sim 10^{14} \text{ m}^{-3}$ ; to  $T \sim 2500$  K,  $n_e \sim 10^{17} \text{ m}^{-3}$  corresponds; and so on.

From the constraint of the self-consistency of the electron concentration and carbon-cluster charges, electron concentration  $n_e(T)$  in carbon-helium plasma was calculated for different temperatures (Fig. 4), that is, in the absence of any other source of electrons or ions other than carbon clusters.

In addition to the plot of self-consistent electron concentration, Fig. 4 shows equal-value lines for the one-stage  $C_{60}$  assembling rate (Fig. 2, surface 1). Figure 4 makes it clear that the peak  $C_{60}$  assembling rate at some temperature corresponds to the electron concentration of pure carbon-helium plasma at this temperature. From this correspondence, the following important inference can be made: the maximal fullerene yield in the arc-plasma discharge is achievable precisely in pure carbon-helium plasma free of any electron donors or acceptors.

The existence of optimal plasma parameters for  $C_{60}$  synthesis can be explained by the strong dependence of the mean carbon-cluster charge on temperature. This dependence is illustrated by Fig. 5.

$$n_e(T) = \sum_m \sum_{q_m=-2}^{+1} n_m(q_m), \quad (12)$$

where  $n_m(q_m)$  is the concentration of carbon clusters  $C_m$  that carry charge  $q_m$ , which is a function of  $n_e$  and  $T$ .

For the temperature and electron concentration that correspond to the maximal  $C_{60}$  assembling rate, the charges on clusters  $C_2$  and  $C_{58}$  are high enough and have opposite signs (for  $T \sim 2000$  K and  $n_e \sim 10^{14} \text{ m}^{-3}$ ,

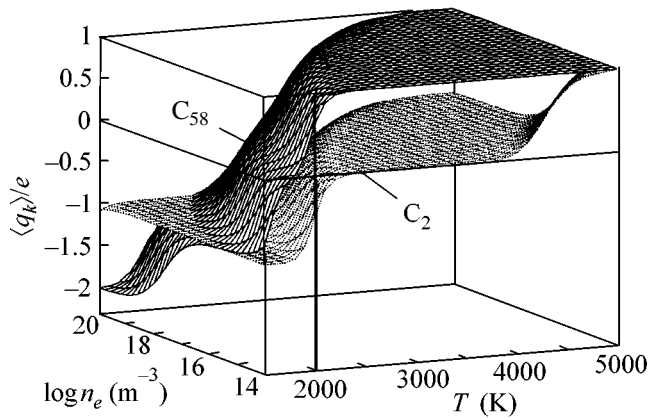


Fig. 5. Charges on clusters  $C_2$  and  $C_{58}$ .

the charges are  $-0.5$  and  $+0.6$ , respectively). As a result, the collision rate of these clusters is several times higher than in adjacent domains, and the  $C_{60}$  assembling rate increases in association.

This work was financially supported by the INTAS grant no. 01-2399, the State Scientific and Engineering Program "Topical Lines of Research in Condensed Matter Physics" (project no. 5-3-00), and the Program "Priority Scientific and Engineering Research in Higher Education Institutions" (project no. 05.01.001).

#### REFERENCES

1. Yu. E. Lozovik and A. M. Popov, *Usp. Fiz. Nauk* **167**, 751 (1997) [*Phys. Usp.* **40**, 717 (1997)].

2. D. V. Afanas'ev, G. A. Dyuzhev, and V. I. Karataev, *Pis'ma Zh. Tekh. Fiz.* **25** (5), 35 (1999) [*Tech. Phys. Lett.* **25**, 182 (1999)].
3. N. I. Alekseev and G. A. Dyuzhev, *Zh. Tekh. Fiz.* **69** (12), 42 (1999) [*Tech. Phys.* **44**, 1435 (1999)].
4. N. A. Vatolin, E. A. Kibanova, and V. A. Polukhin, *Dokl. Akad. Nauk* **356**, 57 (1997).
5. D. M. Cox, K. C. Reichmann, and A. Kaldor, *J. Chem. Phys.* **88**, 1588 (1988).
6. O. A. Nerushev and G. I. Sukhinin, *Zh. Tekh. Fiz.* **67** (2), 41 (1997) [*Tech. Phys.* **42**, 160 (1997)].
7. G. N. Churilov, A. S. Fedorov, and P. V. Novikov, *Carbon* (in press).
8. E. Hernandez, P. Ordejon, and H. Terrones, *Phys. Rev. B* **63**, 193403 (2001).
9. M. Mitchner and C. H. Kruger, Jr., *Partially Ionized Gases* (Wiley, New York, 1973; Mir, Moscow, 1976).
10. L. D. Landau and E. M. Lifshitz, *Course of Theoretical Physics, Vol. 1: Mechanics* (Nauka, Moscow, 1973; Pergamon, New York, 1988).
11. G. N. Churilov, P. V. Novikov, V. E. Taraban'ko, *et al.*, *Carbon* **40**, 891 (2002).
12. P. A. Redhead, *Vacuum* **12**, 203 (1962).
13. G. Kresse and J. Furthmuller, *Comput. Mater. Sci.* **6**, 15 (1996).
14. G. Kresse and J. Furthmuller, *Phys. Rev. B* **54**, 11169 (1996).
15. D. Vanderbilt, *Phys. Rev. B* **41**, 7892 (1990).

Translated by O. Fedorova